

1 **Comparison of Solvent Extraction and Extraction Chromatography Resin**
2 **Techniques for Uranium Isotopic Characterization in High-Level Radioactive**
3 **Waste and Barrier Materials**

4
5 Santiago Hurtado-Bermúdez¹, María Villa-Alfageme², José Luis Mas³, María Dolores
6 Alba⁴

7
8 ¹*Centro de Investigación Tecnología e Innovación, Universidad de Sevilla (CITIUS). Av.*
9 *Reina Mercedes 4B. 41012 Sevilla, Spain*

10 ²*Dpto. Física Aplicada II, ETSIE. Av. Reina Mercedes 4A. Universidad de Sevilla.*
11 *41012-Sevilla, Spain*

12 ³*Dpto. Física Aplicada I, Escuela Universitaria Politécnica. Universidad de Sevilla,*
13 *Spain*

14 ⁴*Instituto Ciencia de los Materiales de Sevilla, CSIC-Universidad de Sevilla, Avda,*
15 *Américo Vespucio, 49, Sevilla, Spain*

16
17 **Abstract**

18 The development of Deep Geological Repositories (DGP) to the storage of high-level
19 radioactive waste (HLRW) is mainly focused in systems of multiple barriers based on the
20 use of clays, and particularly bentonites, as natural and engineered barriers in nuclear
21 waste isolation due to their remarkable properties.

22 Due to the fact that uranium is the major component of HLRW, it is required to go in
23 depth in the analysis of the chemistry of the reaction of this element within bentonites.

24 The determination of uranium under the conditions of HLRW, including the analysis of
25 silicate matrices before and after the uranium-bentonite reaction, was investigated. The
26 performances of a state-of-the-art and widespread radiochemical method based on
27 chromatographic UTEVA resins, and a well-known and traditional method based on
28 solvent extraction with tri-n-butyl phosphate (TBP), for the analysis of uranium and
29 thorium isotopes in solid matrices with high concentrations of uranium were analysed in
30 detail.

31 In the development of this comparison, both radiochemical approaches have an
32 overall excellent performance in order to analyse uranium concentration in HLRW
33 samples. However, due to the high uranium concentration in the samples, the
34 chromatographic resin is not able to avoid completely the uranium contamination in the
35 thorium fraction.

36 **Keywords**

37 high-level radioactive waste; UTEVA; TBP; uranium; thorium

38 **1. Introduction**

39 Many researchers are devoted to the development of Deep Geological Repositories
40 (DGP) to the storage of high-level radioactive waste (HLRW). Mainly the selected
41 solution is based on a system of multiple barriers. Most of security of the disposal relies
42 on an engineered barrier. Clays are ideal materials for natural and engineered barriers for
43 nuclear waste isolation due to their high sorption capacity, low permeability, and swelling
44 capability. In experimental conditions, it is found that the radioactive wastes are
45 immobilised and their diffusion prevented through physical-chemical mechanism with a
46 clay barrier, such as precipitation, adsorption or a chemical reaction including the
47 formation of secondary stable mineral phases. At present, bentonite is established as the
48 most appropriate clay to form the engineered barrier in the DGP (Kaufhold et al., 2015).

49 Previous papers have analysed the capacity of retention and the kinetics reaction
50 properties of bentonites in relation to several radionuclides such as ^{152}Eu (Alba et al.,
51 2011; Mrabet et al., 2014; Villa-Alfageme et al., 2014), additionally trivalent simulators
52 of actinides have been used to study their potential retention capacity of HLRW by
53 bentonites (Alba et al., 2009; Alba and Chaín, 2007). Determination of radionuclides in
54 HLRW is important for nuclear waste management. Because uranium is the major
55 component of HLRW, it is required to go in depth in the analysis of the chemistry of this
56 element within bentonites and other clays and for this, specific radiochemical methods
57 must be developed. Additionally, uranium undergoes a decay chain containing several
58 radioactive isotopes, such as thorium and polonium, that have also to be analysed within
59 HLRW.

60 A complete control of the geochemical behaviour of uranium under the specific
61 conditions created by HLRW includes the analysis of silicate matrices before and after
62 the uranium-bentonite reaction. Because this step is crucial when performing a complete
63 study of the reaction properties of the system uranium-bentonite. It is then key to develop
64 suitable methods for this kind of determinations.

65 Among the methods proposed in the literature to determine uranium in several matrices,
66 the most recent ones are focused on behaviour of selected fission products and actinides
67 on UTEVA resin (Skinner and Knight, 2016), purification of uranium using *n*-tri butyl
68 phosphate (TBP) as extractant and *n*-decanol as phase modifier (Pradeep and Biswas,
69 2017), extraction of uranium from simulated highly active feed in a micromixer-settler
70 with 30% TBP and 36% TiAP solvents (Kumar et al., 2017), diluted salts by TBP and
71 dialkyl amides (Ansari et al., 2016), or uranyl selective polymeric membrane electrodes
72 (Badr et al., 2014). However, it is not analysed the suitability and the sensitivity of
73 currently available radiochemical methods when uranium must be quantified in complex
74 matrices related to HLRW.

75 For this reason, in this study the performances of one state-of-the-art and widespread
76 radiochemical method for the analysis of uranium (and additionally thorium and
77 polonium) isotopes in solid matrices (Mas et al., 2012) was analysed in detail when it is

78 applied to the measurement of matrices with high concentrations of uranium. This
79 method combines a sequential separation of polonium-thorium-uranium using
80 chromatographic UTEVA (Triskem Int.) resins and alpha spectrometry as radiometric
81 measurement method. Additionally, a well-known and traditional method was used to
82 compare the performance of the UTEVA resins. In that case, uranium and thorium were
83 extracted using tri-n-butyl phosphate (TBP) as solvent extraction method, combined with
84 AG1-X8 ion-exchange resin (Villa et al., 2011). This method has the main drawback that
85 is time consuming, but is a routine and robust method to extract uranium, thorium and
86 plutonium as part of the nuclear reprocessing process (Dey and Bansal, 2006).

87 The analysed matrices were uranyl nitrates, and bentonites after a hydrothermal treatment
88 with uranyl nitrate. The main objective of this paper is to analyse the performance of the
89 UTEVA method to be used as a routine method to evaluate uranium, and additionally
90 thorium and polonium, in HLRW samples, where high uranium concentrations are
91 expected.

92 **2. Experimental**

93 *2.1. Sample preparation*

94 In the comparative study between both radiochemical methods, a simulated HLW
95 material was prepared by using two different matrices: uranyl nitrate 6-hydrate
96 $\text{UO}_2(\text{NO}_3)_2 \cdot 6\text{H}_2\text{O}$ (supplied by Panreac) and FEBEX bentonite (from the Cortijo de
97 Archidona deposit, Almería, Spain) (Enresa, 2000). Eight aliquots of this simulated HLW
98 material were prepared and arranged in two groups.

99 In a first group, four aliquots of 0.0048 g of pure uranyl (0.0022 g of uranium) were
100 analysed. ^{232}U , ^{229}Th and ^{209}Po were initially added to the aliquots as internal tracers. The
101 first two aliquots (U-UTEVA-1 and U-UTEVA-2) were analysed following the UTEVA
102 procedure later described, and only the second two aliquots (U-TBP-1 and U-TBP-2)
103 were analysed following the TBP extraction procedure because it is a well-established
104 method that we use as standard method of analysis.

105 In a second group, a total of four aliquots were prepared to check the performance of
106 UTEVA chromatographic resin. ^{232}U was added as internal tracer to those four aliquots in
107 order to quantify uranium separation through UTEVA columns and subsequent alpha
108 spectrometry measurement. First, two aliquots of uranyl nitrate were prepared containing
109 0.55 g of pure uranyl (corresponding to 0.260 g of uranium), and labelled as URANYL-1
110 and URANYL-2. These results were checked against the previous results from the first
111 group of aliquots.

112 Second, two aliquots were prepared by the hydrothermal reaction of 0.032 g of uranyl
113 (0.015 g of uranium) with 300 g FEBEX bentonite and 1.1 g of $\text{ZrO}(\text{NO}_3)_2 \cdot 7\text{H}_2\text{O}$ (as
114 tetravalent simulator of uranium) (Villa-Alfageme et al., 2014). After the hydrothermal
115 reaction, the solid and liquid remnant were examined. The solid product aliquot contained
116 reacted bentonite, zircon silicate and reacted uranium in both phases (labelled as ZrU-
117 Solid) (Villa-Alfageme et al., 2015). The liquid product aliquot contained dissolved
118 zircon and uranium (labelled as ZrU-Liquid). Additionally, in order to validate the
119 analysis of the two aliquots (ZrU-Solid and ZrU-Liquid), a comparison with gamma-ray
120 spectrometry technique was carried on.

121 2.2. *UTEVA chromatographic extraction method*

122 This procedure was adapted from (Mas et al., 2012) for the matrices described and it is
123 schematized in Fig. 1a.

124

125 1. *Digestion of the solid matrix.* Uranyl samples were digested with concentrated
126 nitric acid. Whereas bentonites were total digested by a combination of
127 HNO_3 - HCl - HF (5 mL - 2 mL - 1 mL). Samples were gently heated and stirred
128 until complete dissolution and taken to dryness. Residue is again dissolved in
129 15 mL of 8 mol L^{-1} nitric acid.

- 130 2. Fe^{3+} carrier was added and pH raised to 8.5 with ammonium hydroxide to get
131 the precipitation of iron hydroxides and actinides, the supernatant was
132 removed by siphoning and discarded after settling for at least 8 h.
- 133 3. UTEVA column was preconditioned loading 3.5 mL of 3 mol L⁻¹ HNO₃ three
134 times.
- 135 4. Precipitate was dissolved in 15 mL of 3 mol L⁻¹ HNO₃ - 1 mol L⁻¹ Al(NO₃)₃
136 and 200 mg ascorbic acid. Dissolved sample was loaded into the resin.
- 137 5. *Elution of Am/Pu/Sr/Po/Ra.* The column was rinsed with 5 mL of 3 mol L⁻¹
138 HNO₃ - 1 mol L⁻¹ Al(NO₃)₃, afterwards with 10 mL of 3 mol L⁻¹ HNO₃ three
139 times and finally rinsed with 5 mL of 9 mol L⁻¹ HCl (Oliveira and Carvalho,
140 2006).
- 141 6. *Elution of thorium.* Column was rinsed with 4 mL of 5 mol L⁻¹ HCl - 0.05 mol
142 L⁻¹ oxalic acid five times eluting the thorium fraction.
- 143 7. *Elution of uranium.* The column was finally rinsed with 5 mL of 1 mol L⁻¹
144 HCl three times eluting the uranium fraction.

145 2.3. *TBP liquid-liquid solvent extraction method*

146 The procedure followed for the uranium, thorium and polonium separation was adapted
147 from the TBP procedure described in (Martínez-Aguirre, A., García-León, M., Ivanovich,
148 1994). It is outlined in Fig. 1b and is in detail below:

149

- 150 1. Pretreatment of the sample was carried out following step 1 described in 2.2.
- 151 2. Uranium was precipitated with iron hydroxide and then taken to dryness.
- 152 3. The precipitate was dissolved in 10 mL of 8 mol L⁻¹ HNO₃ and introduced
153 into a 50 mL funnel for the solvent extraction.

- 154 4. 5 mL TBP were added to the funnel.
- 155 5. *Extraction of polonium.* The funnel was shaken for 15 min and the aqueous
156 phase removed. Additionally, 10 mL of 8 mol L⁻¹ HNO₃ were added and the
157 process repeated. This was repeated three times to get an aqueous final
158 solution of 30 mL containing the polonium.
- 159 6. 20 mL Xilene were added to the funnel.
- 160 7. *Extraction of thorium.* 15 mL of 1.5 mol L⁻¹ HCl were added to the funnel and
161 the solution shaken for 10 minutes. The aqueous phase was removed and the
162 process was repeated three times to finally obtain 45 mL of HCl solution,
163 containing thorium (including eventually some traces of uranium).
- 164 8. *Extraction of uranium.* 15 mL of MiliQ water were added and the solution
165 was shaken for 10 minutes. The aqueous phase was removed and the process
166 was repeated again three times to get 45 mL of H₂O solution, containing the
167 uranium fraction.
- 168 9. *Purification of thorium.* Thorium solution obtained from the solvent extraction
169 might present traces of uranium, for this reason it was essential to make a
170 final purification of thorium. This was done by chromatographic separation.
171 6.5 mL of AG1-X8 resin was preconditioned adding 10 mL 9 mol L⁻¹ of HCl
172 twice. Thorium solution was taken to dryness, redissolved in 4 x 10 mL of 9
173 mol L⁻¹ HCl and loaded into the resin. Resin was rinsed three times with 10
174 mL of 9 mol L⁻¹ HCl. Uranium was retained by the resin and a purified Th
175 fraction was obtained after the rinsing.

176 2.4. *Alpha-particle spectrometry*

177 Purified uranium and thorium phases were electroplated onto stainless steel discs
178 (Martínez-Aguirre, A., García-León, M., Ivanovich, 1994) and measured and polonium
179 was self-deposited onto a silver disk (Le Moigne et al., 2013). Counting of thorium,

180 uranium (electro-deposited) and polonium (self-deposited) isotopes was done using alpha
181 detector PIPS type (Canberra) in an array comprised of 10 chambers. Measurements were
182 undertaken at CITIUS (Centro de Investigación, Tecnología e Innovación, Universidad
183 de Sevilla) laboratory at Universidad de Sevilla. The resolution of the peaks was found to
184 be between 60 and 40 keV in all cases.

185 2.5. *Gamma-ray spectrometry*

186 The gamma-ray measurements were carried on by a Canberra n-type hyper-pure
187 germanium gamma-ray detector (HPGe), located at Centro de Investigación, Tecnología
188 e Innovación Universidad de Sevilla, CITIUS, with a nominal relative photo-peak
189 efficiency of 60% at 1332 keV. The detector chamber was set up by a lead shield (10 cm
190 thick standard lead) and an inner copper layer (5 mm) protecting the detector against
191 environmental background radiation. The electronic chain consisted of a Canberra
192 preamplifier 2002, and a Canberra Inspector 2000 DSP digital electronic chain. Gamma-
193 ray spectra were analysed with Genie2K software.

194 Hydrothermal reaction products were collected by filtration using 0.45 µm Milipore
195 filters and air-dried at 60 °C. In order to measure natural ²³⁵U activity in the sample, the
196 gamma-ray emission of 143.8 keV (10.9% total yield) was selected.

197 Counting efficiency were calculated through Monte Carlo simulations using LABSOCS
198 program (Hurtado and Villa, 2010) for the two counting geometries used: a 0.45 µm
199 Millipore filter (ZrU-Solid) and a 100 mL cylindrical beaker (ZrU-Liquid). The
200 composition of the solid sample was essential to compute correctly the simulated
201 efficiency of this counting geometry.

202 Finally, Monte Carlo efficiencies were successful compared to the experimental ones
203 obtained through the preparation of solid and aqueous standards spiked with a known
204 amount of diluted uranyl solution.

205 2.6. *Scanning electron microscopy*

206 The morphology and chemical composition of the hydrothermal products were
207 investigated using a SEM-FEG HITACHI S-4800 a scanning electron microscope
208 equipped with an Xflash 4010 (BRUKER) for energy dispersive X-ray (EDX) analysis,
209 located at Microscopy Service in ICMS (CSIC-Universidad de Sevilla).

210 **3. Results and discussion**

211 In this section, the obtained activities and isotopic ratios using both radiochemical
212 methods are shown for each isotope fraction, and a discussion about the chemical
213 recovery, cross-contamination, and maximum load capacity is carried out.

214 *3.1. Uranium fractions*

215 The results obtained for uranium activity for each aliquot and radiochemical method
216 (TBP or UTEVA) are presented in Table 1 and Fig. 2. The components contributing to
217 the combined measurement uncertainty such as count rates of sample and tracer,
218 chemical recovery, tracer activity and mass of the sample and the tracer are calculated as
219 one standard deviation.

220 Table 1 shows that both UTEVA column method and TBP method are capable of
221 extracting the uranium from the analysed aliquot with an acceptable chemical yield. The
222 chemical yield using the added ^{232}U internal tracer is around 45% for the solvent
223 extraction method and 65% for the chromatographic extraction method.

224 With respect to the isotopic ratios, the values obtained for ^{234}U and ^{238}U ($^{234}\text{U}/^{238}\text{U}$), and
225 ^{235}U and ^{238}U ($^{235}\text{U}/^{238}\text{U}$) are 0.45 and 0.095 respectively. These values do not correspond
226 to those of natural uranium, ~ 1 and 0.046 respectively (Brennecka et al., 2010). However,
227 this is in agreement with the values measure in commercial uranium reagents (Iturbe,
228 1992). Specifically, the $^{234}\text{U}/^{238}\text{U}$ isotopic ratio for U-UTEVA-2 sample is 20% lower
229 than the ratios obtained for U-TBP-1, U-TBP-2 and U-UTEVA-1 samples, and it is also
230 40% higher for the $^{235}\text{U}/^{238}\text{U}$ ratio (see Table 1). It can be asserted that this behaviour is
231 not due to the pre-treatment because this step is common for samples U-TBP-1, U-TBP-
232 2, U-UTEVA-1 and UTEVA-2. This effect has not been observed in the analysis of

233 environmental samples following UTEVA method. Further studies should be conducted
234 in that respect.

235 On the other hand, thorium was not detected in any of the two methods in the
236 electrodeposited U fraction. Since thorium concentration is very small in uranyl matrices,
237 thorium contamination in U fraction was evaluated from the analysis of ^{229}Th tracer.

238 One of the drawbacks of the use of UTEVA resins for uranium analysis is its limitation
239 on the maximum accepted uranium concentration and its dependence on the type of
240 matrix. The manufacturer recommends a maximum load capacity of the UTEVA resin
241 (Triskem Int.) for U is approximately 0.015 g per 2 mL of the pre-packaged UTEVA
242 columns. In order to check the UTEVA performance several experiments were carried
243 out using only UTEVA columns for the analysis of two aliquots of pure uranyl
244 (URANYL-1, URANYL-2). In the experiments with pure uranyl the maximum capacity
245 of the column for the measurement of U was exceeded, since 0.260 g of uranyl was
246 analysed. The results in Table 2 show that the chemical yields drop below 1% when
247 exceeding the capacity of the column. These results indicate that for UTEVA method it is
248 very important not exceed the load capacity, because the chemical yield decreases
249 drastically, and therefore, an increase of the resin weight required to analyse samples
250 with high concentration of uranium is cost-prohibitive.

251 Additionally, as in most analytical situations, the presence of significant concentrations
252 of matrix elements can affect the proper operation of methods based on UTEVA resin
253 (Horwitz et al., 1992). Therefore, the performance of these resins was evaluated also in
254 matrices with high silicate content (high refractory fraction). In order to check the
255 UTEVA performance several experiments were carried out using only UTEVA columns
256 for the analysis of two aliquots of zirconium-uranium disilicate, formed after a
257 hydrothermal treatment with FEBEX and $\text{ZrO}(\text{NO}_3)_2\text{-UO}_2(\text{NH}_3)_2$ (Villa-Alfageme et al.,
258 2015), containing the solid fraction (ZrU-Solid) and the liquid one (ZrU-Liquid) (see
259 Section 2.1. for description).

260 The characterization of the solid fraction was carried out through SEM micrographs of
261 the reacted FEBEX with ZrO^{2+} (Fig. 3). The solid sample shows lamellar particles with a

262 chemical composition consisting mainly of ZrO^{2+} as interlayer cations (Figs. 3a–3d), and
263 agglomerations of small particles with brilliant appearance (Fig. 3b, point 1) with a
264 chemical composition compatible with phase containing zirconium (Fig. 3e). Moreover,
265 the SEM/EDX analysis of a different zone (Fig. 3c, point 2) indicated that the treated clay
266 mineral contain iron, probably released upon degradation of the container (Fig. 3f).

267 Finally, the ZrU-Solid and ZrU-Liquid samples were analysed using both UTEVA
268 radiochemical method and alpha-particle spectrometry, and gamma-ray spectrometry
269 technique. This all translates in the results shown in Table 2. The activity of ^{235}U for
270 ZrU-Solid and ZrU-Liquid samples through gamma-ray spectrometry was 7.6 ± 1.5 Bq
271 and 3.5 ± 1.4 Bq respectively. Both methods give results in total agreement validating the
272 use of UTEVA resin for the analysis of complex matrices.

273

274 3.2. *Thorium fractions*

275 The results obtained for the concentrations of thorium activity for each aliquot and
276 radiochemical method are presented in Table 3.

277 Natural thorium is not measured in the Th fraction above the limit of detection through
278 any of the radiochemical methods. The chemical yields obtained through ^{229}Th are
279 similar to those obtained for the U fraction. According to the obtained thorium yields,
280 both methods are apparently suitable for Th measurements.

281 However, the percentage of U in the Th fraction of the analysed samples has been
282 obtained and shown in Fig. 4. Note that a significant difference between the two methods
283 (UTEVA and TBP) is shown in relation to the Th detected. In the samples separated by
284 UTEVA chromatography columns (U-UTEVA-1 and U-UTEVA-2), U isotopes peaks
285 clearly appear in the Th fraction contaminating the results. The contamination of U has
286 been possibly detected because the analysed samples were high activity samples (about
287 10 Bq). This contamination of U in the Th fraction is not usually observed in the analysis
288 of low-level environmental samples by UTEVA method because the percentage of the
289 initial U activity presented in the spectra of Th was calculated to be a 1.5%

290 approximately. On the other hand, this contamination does not exist in the samples
291 separated by the TBP solvent extraction method.

292 Therefore, the U-Th separation procedure using UTEVA columns efficiently separates
293 the Th fraction from uranium, but about 1.5% of the initial uranium contaminates the Th
294 fraction (Mas et al., 2012). This is especially relevant in those matrices where the activity
295 of U is at least one order of magnitude higher than the activity of Th.

296 3.3. *Polonium fraction*

297 The results obtained for the concentrations of polonium activity for each aliquot and
298 radiochemical method are presented in Table 4. Radiochemical yields around 55-60% are
299 obtained for both methods using ^{209}Po as tracer.

300 It must be highlighted the need to place the silver disk vertically during the
301 autodeposition process, and finally washing it with acetone and distilled water to avoid
302 the deposition of U traces on the disk. This is important in this case due to the very high
303 concentration of uranium in the sample.

304 Finally, traces of natural ^{210}Po in uranyl samples were detected. The origin is the decay
305 chain of ^{238}U . However, high uncertainties for the activities are obtained because these
306 activities are very close to the minimum detectable activity.

307 4. Conclusions

308 The standard TBP method has proven to be an efficient and robust technique to analyse
309 uranium and thorium concentration for all kinds of samples (either HLRW or low-level
310 environmental samples). On the other hand, the uranium-thorium separation method
311 using UTEVA columns works efficiently even applied in complex matrices. However,
312 UTEVA radiochemical method reaches a total separation of the uranium fraction from
313 thorium fraction, but a maximum of 1.5% of the initial uranium contaminates the Th
314 fraction. This is especially relevant in those matrices where the concentration of U is

315 orders of magnitude higher than that of Th. Therefore, further studies should be carried
316 out to elucidate the use of UTEVA resins in the analysis of HLRW materials.

317 **Acknowledgements**

318 We would like to thank to ENRESA (contract nº 0079000237) and to the Spanish State
319 Program R+D +I oriented societal challenges and FEDER (Project MAT2015-63929-R)
320 for financial support.

321

322

323

324

325

326

327

328

329

330

331

332

333 Tables

334

335 **Table 1.** Activity (Bq) and isotopic ratios of the uranium isotopes using the
336 radiochemical method with TBP (U-TBP-1 and U-TBP-2) and the radiochemical method
337 with UTEVA (U-UTEVA-1 and U-UTEVA-2). MDA is the Minimum Detectable
338 Activity.

Sample	^{234}U (Bq)	$\pm \sigma$	^{235}U (Bq)	$\pm \sigma$	^{238}U (Bq)	$\pm \sigma$
U-TBP-1	10.8	0.3	2.19	0.07	23.6	0.7
U-TBP-2	10.7	0.3	2.18	0.07	23.4	0.7
U-UTEVA-1	9.9	0.3	2.18	0.07	22.1	0.7
U-UTEVA-2	9.0	0.3	3.25	0.10	23.9	0.7
Sample	$^{234}\text{U}/^{238}\text{U}$	$^{235}\text{U}/^{238}\text{U}$	^{232}U recovery	MDA ^{234}U (Bq)	MDA ^{235}U (Bq)	MDA ^{238}U (Bq)
U-TBP-1	0.46	0.093	44%	0.05	0.08	0.06
U-TBP-2	0.46	0.093	47%	0.05	0.07	0.06
U-UTEVA-1	0.45	0.099	63%	0.04	0.08	0.05
U-UTEVA-2	0.38	0.136	65%	0.05	0.09	0.05

339

340

341

342

343

344

345

346

347

348

349

350

351 **Table 2.** Activity (Bq) and isotopic ratios (in activity) of the uranium isotopes using the
 352 UTEVA radiochemical method for pure uranyl matrices (URANYL-1 and URANYL-2)
 353 and the product of a hydrothermal treatment with FEBEX and $\text{ZrO}(\text{NO}_3)_2\text{-UO}_2(\text{NH}_3)_2$ in
 354 the solid fraction (ZrU-Solid) and liquid (ZrU-Liquid). Chemical yields are not included
 355 for samples under hydrothermal treatment, since most of the uranium is lost in that
 356 process, not during the radiochemical procedure. MDA is the Minimum Detectable
 357 Activity.

Sample	^{234}U (Bq)	$\pm \sigma$	^{235}U (Bq)	$\pm \sigma$	^{238}U (Bq)	$\pm \sigma$
URANYL-1	666	79	144	17	1541	183
URANYL-2	548	92	78	13	1120	189
ZrU-Solid	52.9	2.4	7.9	0.4	109.3	5.0
ZrU-Liquid	16.1	4.6	3.0	0.7	36.2	7.1
Sample	$^{234}\text{U}/^{238}\text{U}$	$^{235}\text{U}/^{238}\text{U}$	^{232}U recovery	MDA ^{234}U (Bq)	MDA ^{235}U (Bq)	MDA $^{238}\text{U}/$ (Bq)
URANYL-1	0.432	0.0938	0.54%	0.05	0.08	0.06
URANYL-2	0.489	0.0695	0.30%	0.05	0.07	0.06
ZrU-Solid	0.485	0.0723	--	0.04	0.08	0.05
ZrU-Liquid	0.446	0.0830	--	0.05	0.09	0.05

358

359

360

361

362

363

364

365

366 **Table 3.** Activity (Bq) of thorium isotopes using the radiochemical procedure with TBP
367 (U-TBP-1 and U-TBP-2) and the radiochemical process with UTEVA (U-UTEVA-1 and
368 U-UTEVA-2). The chemical recovery is shown through ^{229}Th . MDA is the Minimum
369 Detectable Activity.

Sample	^{230}Th (Bq)	$\pm \sigma$	^{232}Th (Bq)	$\pm \sigma$	^{229}Th recovery	MDA ^{230}Th (Bq)	MDA ^{232}Th (Bq)
U-TBP-1	<MDA		<MDA		60	0.12	0.06
U-TBP-2	<MDA		<MDA		52	0.04	0.05
U-UTEVA-1	<MDA		<MDA		71	0.07	0.03
U-UTEVA-2	<MDA		<MDA		51	0.05	0.05

370

371

372

373

374

375

376

377

378

379

380

381

382

383

384 **Table 4.** Activity (Bq) of ^{210}Po using the radiochemical procedure with TBP (U-TBP-1
385 and U-TBP-2) and the chemical procedure with UTEVA (U-UTEVA-1 and U-UTEVA-
386 2). MDA is the Minimum Detectable Activity.

Sample	^{210}Po (Bq)	$\pm \sigma$	MDA (Bq)
U-TBP-1	0.00025	0.00013	0.00024
U-TBP-2	0.00064	0.00017	0.00021
U-UTEVA-1	0.00069	0.00017	0.00016
U-UTEVA-2	0.00045	0.00011	0.00016

387

388

389

390

391

392

393

394

395

396

397

398 Table captions

399 **Table 1.** Activity (Bq) and isotopic ratios of the uranium isotopes using the
400 radiochemical method with TBP (U-TBP-1 and U-TBP-2) and the radiochemical method
401 with UTEVA (U-UTEVA-1 and U-UTEVA-2). MDA is the Minimum Detectable
402 Activity.

403 **Table 2.** Activity (Bq) and isotopic ratios (in activity) of the uranium isotopes using the
404 UTEVA radiochemical method for pure uranyl matrices (URANYL-1 and URANYL-2)
405 and the product of a hydrothermal treatment with FEBEX and $\text{ZrO}(\text{NO}_3)_2\text{-UO}_2(\text{NH}_3)_2$ in
406 the solid fraction (ZrU-Solid) and liquid (ZrU-Liquid). Chemical yields are not included
407 for samples under hydrothermal treatment, since most of the uranium is lost in that
408 process, not during the radiochemical procedure. MDA is the Minimum Detectable
409 Activity.

410 **Table 3.** Activity (Bq) of thorium isotopes using the radiochemical procedure with TBP
411 (U-TBP-1 and U-TBP-2) and the radiochemical process with UTEVA (U-UTEVA-1 and
412 U-UTEVA-2). The chemical recovery is shown through ^{229}Th . MDA is the Minimum
413 Detectable Activity.

414 **Table 4.** Activity (Bq) of ^{210}Po using the radiochemical procedure with TBP (U-TBP-1
415 and U-TBP-2) and the chemical procedure with UTEVA (U-UTEVA-1 and U-UTEVA-
416 2). MDA is the Minimum Detectable Activity.

417

418

419

420

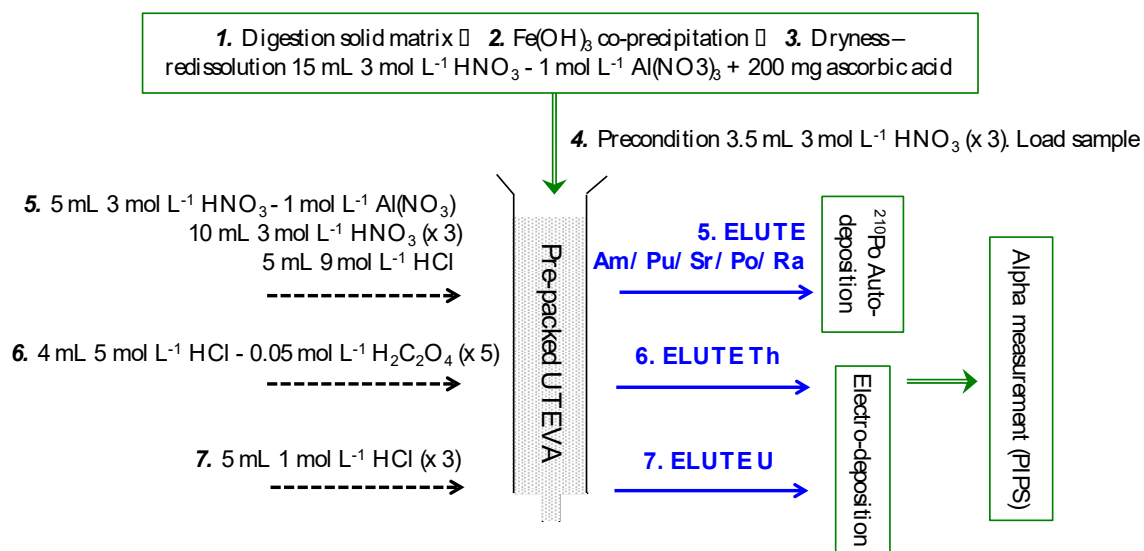
421

422 Figures

423

424

425

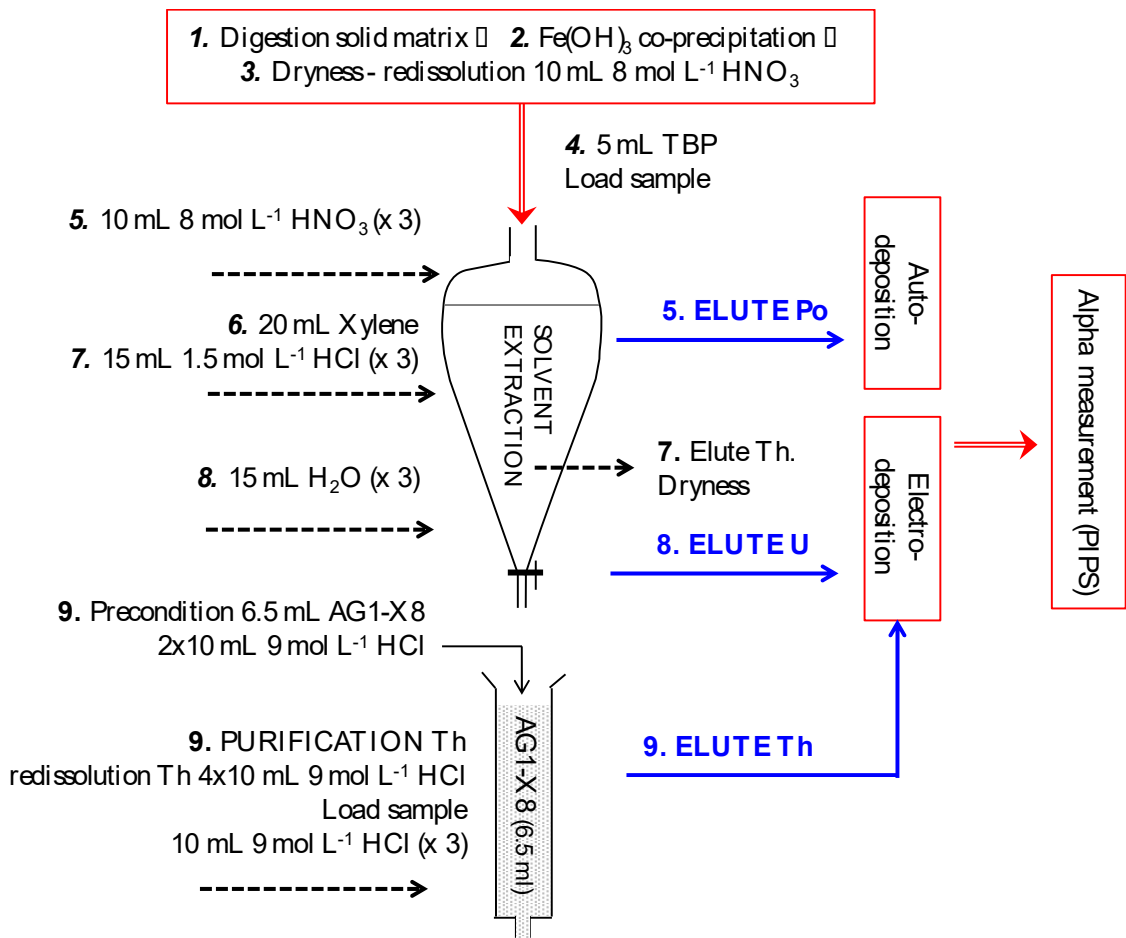


426

427 **Fig. 1a.** UTEVA chromatographic extraction method.

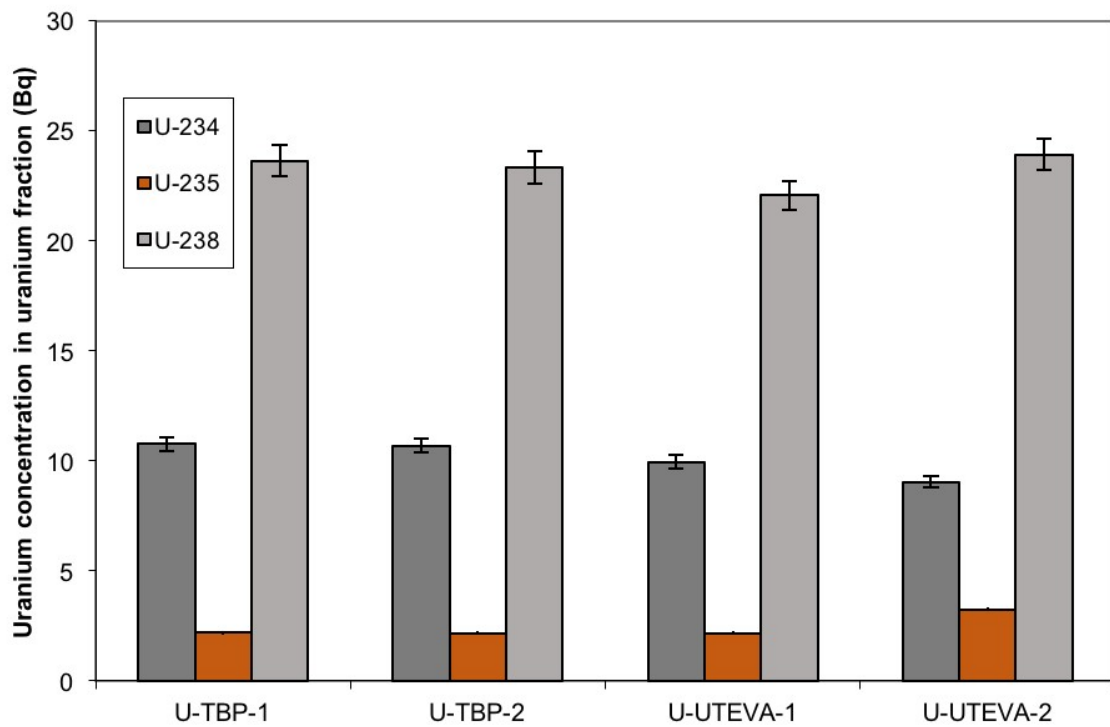
428

429



430

431 **Fig. 1b.** TBP liquid-liquid solvent extraction method.



432

433 **Fig. 2.** Activity concentration (Bq) and isotopic ratios of the uranium isotopes using the
 434 radiochemical method with TBP (U-TBP-1 and U-TBP-2) and the radiochemical method
 435 with UTEVA (U-UTEVA-1 and U-UTEVA-2).

436

437

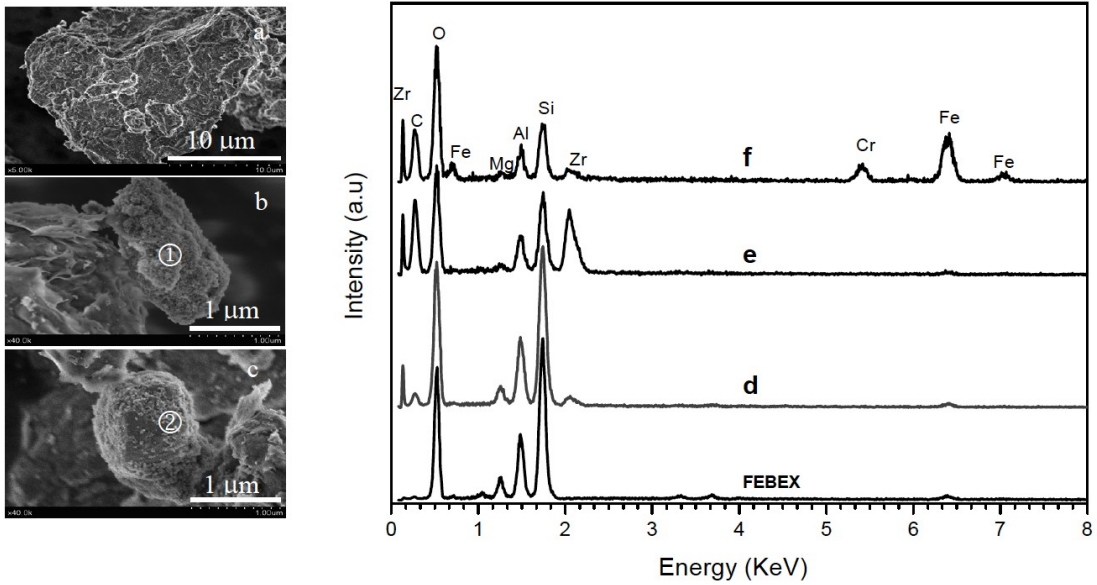
438

439

440

441

442



443

444 **Fig. 3.** SEM micrographs of the reacted FEBEX with a solution of ZrO_2+ : (a) a general
 445 view; (b) bright particles agglomerates mainly made up of zirconium; and (c) iron
 446 particles coming from container degradation. EDX spectra of: (d) lamellar particles; (e)
 447 zirconium agglomerates; (f) iron particles; and a FEBEX spectrum as reference.

448

449

450

451

452

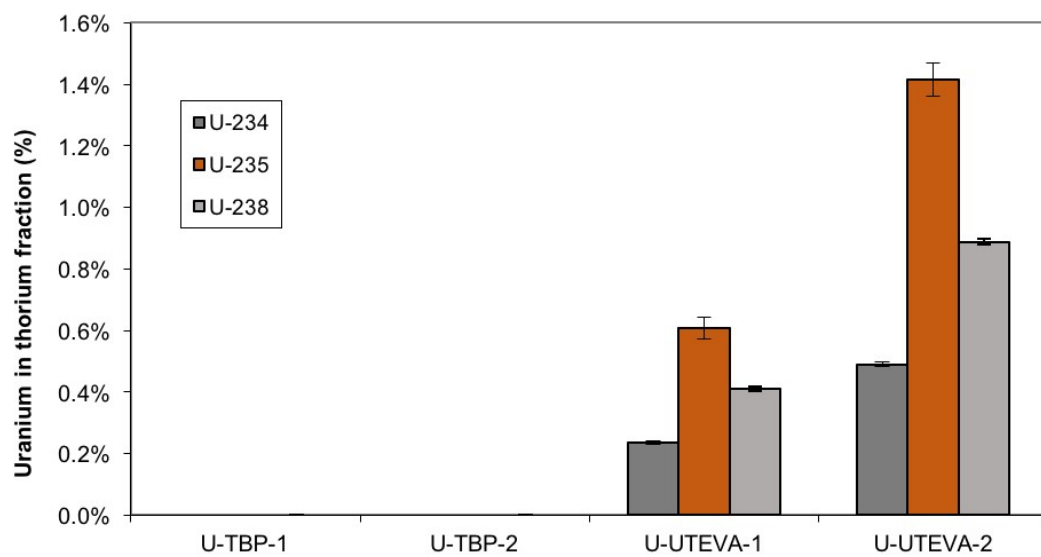
453

454

455

456

457



458

459 **Fig. 4.** Percentage of uranium measured in thorium fraction in uranyl aliquots measured
460 by TBP (U-TBP-1 and U-TBP-2) and UTEVA (U-UTEVA-1 and U-UTEVA-2).

461

462

463

464

465

466

467

468

469

470 Figure captions

471

472 **Fig. 1a.** UTEVA chromatographic extraction method.

473

474 **Fig. 1b.** TBP liquid-liquid solvent extraction method.

475

476 **Fig. 2.** Activity concentration (Bq) and isotopic ratios of the uranium isotopes using the
477 radiochemical method with TBP (U-TBP-1 and U-TBP-2) and the radiochemical method
478 with UTEVA (U-UTEVA-1 and U-UTEVA-2).

479

480 **Fig. 3.** SEM micrographs of the reacted FEBEX with a solution of ZrO_2^{+} : (a) a general
481 view; (b) bright particles agglomerates mainly made up of zirconium; and (c) iron
482 particles coming from container degradation. EDX spectra of: (d) lamellar particles; (e)
483 zirconium agglomerates; (f) iron particles; and a FEBEX spectrum as reference.

484

485 **Fig. 4.** Percentage of uranium measured in thorium fraction in uranyl aliquots measured
486 by TBP (U-TBP-1 and U-TBP-2) and UTEVA (U-UTEVA-1 and U-UTEVA-2).

487

488

489

490

491

492

493

494

References

- 495 Alba, M.D., Castro, M.A., Chaín, P., Hurtado, S., Orta, M.M., Pazos, M.C., Villa, M.,
496 2011. Interaction of Eu-isotopes with saponite as a component of the engineered
497 barrier. *Appl. Clay Sci.* 52, 253–257. doi:10.1016/j.clay.2011.02.027
- 498 Alba, M.D., Chaín, P., 2007. Persistence of lutetium disilicate. *Appl. Geochemistry* 22,
499 192–201. doi:10.1016/j.apgeochem.2006.09.012
- 500 Alba, M.D., Chain, P., Orta, M.M., 2009. Chemical reactivity of argillaceous material in
501 engineered barrier. Rare earth disilicate formation under subcritical conditions.
502 *Appl. Clay Sci.* 43, 369–375. doi:10.1016/j.clay.2008.11.004
- 503 Ansari, S.A., Kumari, N., Raut, D.R., Kandwal, P., Mohapatra, P.K., 2016. Comparative
504 dispersion-free solvent extraction of Uranium(VI) and Thorium(IV) by TBP and
505 dialkyl amides using a hollow fiber contactor. *Sep. Purif. Technol.* 159, 161–168.
506 doi:10.1016/j.seppur.2016.01.004
- 507 Badr, I.H.A., Zidan, W.I., Akl, Z.F., 2014. Cyanex based uranyl sensitive polymeric
508 membrane electrodes. *Talanta* 118, 147–155. doi:10.1016/j.talanta.2013.10.011
- 509 Brennecka, G.A., Borg, L.E., Hutcheon, I.D., Sharp, M.A., Anbar, A.D., 2010. Natural
510 variations in uranium isotope ratios of uranium ore concentrates: Understanding the
511 $^{238}\text{U}/^{235}\text{U}$ fractionation mechanism. *Earth Planet. Sci. Lett.* 291, 228–233.
512 doi:10.1016/j.epsl.2010.01.023
- 513 Dey, P.K., Bansal, N.K., 2006. Spent fuel reprocessing: A vital link in Indian nuclear
514 power program. *Nucl. Eng. Des.* 236, 723–729.
515 doi:10.1016/j.nucengdes.2005.09.029
- 516 Enresa, 2000. FEBEX Project. Full scale engineered barriers experiment for a deep
517 geological repository for high level radioactive waste in crystalline host rock. Final
518 Report. ENRESA Publicaciones técnicas 374.
- 519 Horwitz, E.P., Dietz, M.L., Chiarizia, R., Diamond, H., Essling, A.M., Graczyk, D.,
520 1992. Separation and preconcentration of uranium from acidic media by extraction
521 chromatography. *Anal. Chim. Acta* 266, 25–37. doi:10.1016/0003-2670(92)85276-C
- 522 Hurtado, S., Villa, M., 2010. An intercomparison of Monte Carlo codes used for in-situ
523 gamma-ray spectrometry. *Radiat. Meas.* 45, 923–927.
524 doi:10.1016/j.radmeas.2010.06.001
- 525 Iturbe, J.L., 1992. Identification of ^{236}U in commercially available uranium compounds
526 by alpha particle spectrometry. *Int. J. Radiat. Appl. Instrumentation. Part 43*, 817–
527 818. doi:10.1016/0883-2889(92)90249-E
- 528 Kaufhold, S., Hassel, A.W., Sanders, D., Dohrmann, R., 2015. Corrosion of high-level
529 radioactive waste iron-canisters in contact with bentonite. *J. Hazard. Mater.* 285,
530 464–473. doi:10.1016/j.jhazmat.2014.10.056
- 531 Kumar, S., Kumar, B., Sinha, P.K., Sampath, M., Sivakumar, D., Mudali, U.K., 2017.

532 Extraction of uranium from simulated highly active feed in a micromixer-settler
533 with 30% TBP and 36% TiAP solvents. *J. Radioanal. Nucl. Chem.* 311, 2111–2116.
534 doi:10.1007/s10967-016-5134-5

535 Le Moigne, F.A.C., Villa-Alfageme, M., Sanders, R.J., Marsay, C., Henson, S., García-
536 Tenorio, R., 2013. Export of organic carbon and biominerals derived from ²³⁴Th
537 and ²¹⁰Po at the Porcupine Abyssal Plain. *Deep. Res. Part I Oceanogr. Res. Pap.* 72,
538 88–101. doi:10.1016/j.dsr.2012.10.010

539 Martínez-Aguirre, A., García-León, M., Ivanovich, M., 1994. The Distribution of U, Th
540 and ²²⁶Ra derived from the phosphate fertilizer industries on an estuarine system in
541 Southwes Spain. *J. Environ. Radioact.* 22, 155–177. doi:10.1016/0265-
542 931X(94)90020-5

543 Mas, J.L., Villa, M., Hurtado, S., García-Tenorio, R., 2012. Determination of trace
544 element concentrations and stable lead, uranium and thorium isotope ratios by
545 quadrupole-ICP-MS in NORM and NORM-polluted sample leachates. *J. Hazard.*
546 *Mater.* 205, 198–207. doi:10.1016/j.jhazmat.2011.12.058

547 Mrabet, S. El, Castro, M.A., Hurtado, S., Orta, M.M., Pazos, M.C., Villa-Alfageme, M.,
548 Alba, M.D., 2014. Competitive effect of the metallic canister and clay barrier on the
549 sorption of Eu³⁺ under subcritical conditions. *Appl. Geochemistry* 40, 25–31.
550 doi:10.1016/j.apgeochem.2013.10.014

551 Oliveira, J.M., Carvalho, F.P., 2006. Sequential extraction procedure for determination of
552 uranium, thorium, radium, lead and polonium radionuclides by alpha spectrometry
553 in environmental samples. *Czechoslov. J. Phys.* 56. doi:10.1007/s10582-006-0548-x

554 Pradeep, A., Biswas, S., 2017. Purification of uranium from zirconium-rich crude sodium
555 di-uranate using counter-current solvent extraction. *J. Radioanal. Nucl. Chem.* 313,
556 93–99. doi:10.1007/s10967-017-5291-1

557 Skinner, M., Knight, D., 2016. The behaviour of selected fission products and actinides
558 on UTEVA® resin. *J. Radioanal. Nucl. Chem.* 307, 2549–2555.
559 doi:10.1007/s10967-016-4706-8

560 Villa-Alfageme, M., Hurtado, S., Castro, M.A., El Mrabet, S., Orta, M.M., Pazos, M.C.,
561 Alba, M.D., 2014. Quantification and comparison of the reaction properties of
562 FEBEX and MX-80 clays with saponite: Europium immobilisers under subcritical
563 conditions. *Appl. Clay Sci.* 101, 10–15. doi:10.1016/j.clay.2014.08.012

564 Villa-Alfageme, M., Hurtado, S., El Mrabet, S., Pazos, M.C., Castro, M.A., Alba, M.D.,
565 2015. Uranium immobilization by FEBEX bentonite and steel barriers in
566 hydrothermal conditions. *Chem. Eng. J.* 269, 279–287.
567 doi:10.1016/j.cej.2015.01.134

568 Villa, M., Manjón, G., Hurtado, S., García-Tenorio, R., 2011. Uranium pollution in an
569 estuary affected by pyrite acid mine drainage and releases of naturally occurring
570 radioactive materials. *Mar. Pollut. Bull.* 62, 1521–1529.
571 doi:10.1016/j.marpolbul.2011.04.003

572